

Polarimetric variations of binary stars. III Periodic polarimetric variations of the Herbig Ae/Be star MWC 1080¹

N. Manset² and P. Bastien

Université de Montréal, Département de Physique, and Observatoire du Mont Mégantic, C.P. 6128, Succ. Centre-ville, Montréal, QC, H3C 3J7, Canada

manset@cfht.hawaii.edu, bastien@astro.umontreal.ca

ABSTRACT

We present polarimetric observations of a massive pre-main sequence short-period binary star of the Herbig Ae/Be type, MWC 1080. The mean polarization at 7660 Å is 1.60% at 81.6°, or 0.6% at 139° if an estimate of the interstellar polarization is subtracted. The intrinsic polarization points to an asymmetric geometry of the circumstellar or circumbinary environment while the 139° intrinsic position angle traces the axis of symmetry of the system and is perpendicular to the position angle of the outflow cavity. The polarization and its position angle are clearly variable, at all wavelengths, and on time scales of hours, days, months, and years. Stochastic variability is accompanied by periodic variations caused by the orbital motion of the stars in their dusty environment. These periodic polarimetric variations are the first phased-locked ones detected for a pre-main sequence binary. The variations are not simply double-periodic (seen twice per orbit) but include single-periodic (seen once per orbit) and higher-order variations. The presence of single-periodic variations could be due to non equal mass stars, the presence of dust grains, an asymmetric configuration of the circumstellar or circumbinary material, or the eccentricity of the orbit. MWC 1080 is an eclipsing binary with primary and secondary eclipses occurring at phases 0.0 and 0.55. The signatures of the eclipses are seen in the polarimetric observations.

Subject headings: binaries: close — circumstellar matter — methods: observational — stars: individual (MWC 1080) — stars: pre-main sequence — techniques: polarimetric

1. Introduction

Pre-main sequence (PMS) stars are objects still contracting to the main sequence and generally surrounded by disks and/or envelopes of circumstellar dust and gas, which represent remnant ma-

²Now at: Canada-France-Hawaii Telescope Corporation, P.O. Box 1597, Kamuela, HI 96743, USA

¹Based (in part) on observations collected with the 2m Bernard-Lyot telescope (TBL) operated by INSU/CNRS and Pic-du-Midi Observatory (CNRS USR 5026).

terial from their still-ongoing formation. This circumstellar matter is responsible for phenomena such as emission lines, P Cygni profiles, IR and UV excesses, and polarization. This polarization is produced by scattering on dust grains and has been known for a number of years (see Bastien 1996 for a review).

It is also well known that when a binary star (of any evolutionary status) is surrounded by circumstellar matter, its polarization varies as a function of the orbital period. Some models seek to reproduce these variations (see for example Rudy & Kemp 1978; Brown, McLean, & Emslie 1978) in order to find the orbital inclination of these binary systems. In particular, the work from Brown et al. (1978) (hereafter referred to as BME) uses first and second-order Fourier analysis of the Stokes curves to give, in addition to the orbital inclination, moments related to the distribution of the scatterers in the circumstellar and circumbinary environment.

It could be very interesting to use the BME formalism to find the orbital inclination of PMS binaries, since spectroscopic observations coupled with an orbital inclination can yield the absolute mass of each star. These masses could then be compared with theoretical models of the formation of binary stars, and to masses derived from other types of observations (photometry and theoretical evolutionary tracks for example).

However, the BME formalism was developed for Thomson scattering in optically thin envelopes, and for binaries in circular orbits. Since polarization in PMS stars is produced by scattering on dust grains, and most of the known PMS spectroscopic binaries have eccentric orbits, the BME formalism can not be used a priori. Studies were undertaken to verify the applicability of the BME formalism for Mie scattering and eccentric orbits (see Manset & Bastien 2000, 2001, hereafter referred to as Paper I and II respectively) and have shown that the BME analysis can still be applied in those cases, with a few limitations.

In this context, we have obtained polarimetric observations of 24 PMS spectroscopic binaries, following (with $\gtrsim 10$ observations) the shortest-period ($P \lesssim 35$ d) and brightest ($V \lesssim 12.0$) ones. The observations were used to study the general polarimetric variability of these systems, correlations between these variations and physical characteristics, periodicity in the variations, and to try to determine the orbital inclination.

In this paper, we present the observational method, method of determination of the interstellar polarization, analysis of the polarimetric variability and of the periodic variations, along with data for the only Herbig Ae/Be star of our sample, MWC 1080. The observations and discussion for the rest of the sample will be presented in future papers.

2. Observations

Polarimetric data were taken at the Observatoire du Mont Mégantic (OMM), Canada, with Beauty and The Beast, a two-channel photo-electric polarimeter used at the f/8 Cassegrain focus

of the 1.6m telescope. In this polarimeter, the analyzer is a Wollaston prism which is used in combination with a Pockels cell acting as a variable quarter-wave plate, and an additional quarter-wave plate for linear polarization measurements. See Manset & Bastien (1995) and Manset (2000) for details about the instrument. The high voltage supplied to the Pockels cell is switched at 62.5 Hz to beat down the effects of variable seeing and transparency (Serkowski 1974).

The data were calibrated for instrumental efficiency, instrumental polarization (due to the telescope’s mirrors), and origin of position angles using, respectively, a Glan-Thomson polarizing prism, non-polarized and polarized standard stars. Calibration measurements taken between 1995 and 1999 reveal a very low and stable instrumental polarization under $0.025\% \pm 0.010\%$, and a relatively stable correction for the position angle between -37° and -33° from one observing run to the other.

The observational errors are calculated from photon statistics, but include uncertainties introduced by the polarimetric efficiency of the instrument, the instrumental polarization, and the calibration for the origin of the position angle. The relative errors in position angle can be as low as 0.1° , but due to instrumental effects, systematic errors, and the calibration procedure itself, the absolute errors on the position angles are of the order of 1° . Details on the data reduction, stability of the instrument, and calibrations are given by Manset (2000).

We have also obtained data using the polarimeter STERENN at the 2-meter Bernard-Lyot Telescope of the Observatoire du Pic-du-Midi (OPdM), France. This 2-channel polarimeter uses a half-wave plate rotating at 20 Hz and a Wollaston prism, along with red photo-diodes. Instrumental efficiency is measured with polarized standard stars, and the instrumental polarization, with non-polarized standard stars. The observational errors are calculated from the fit of the observations taken at a frequency of 20 Hz to a sinusoid function.

3. Estimation of the interstellar polarization

Polarimetric observations are in general a sum of intrinsic and interstellar polarizations. It is useful to estimate the importance of interstellar polarization in each measurement made. One can start by looking at the Mathewson et al. (1978) catalog, which contains over 7000 polarimetric observations of bright early-type stars, and compare the level of polarization and position angle of neighboring stars³. However, this can be misleading since interstellar polarization depends on the distance; a target with high polarization could simply be further away and not necessarily intrinsically polarized.

Therefore, for each observed PMS binary, the catalog was scanned to select at least 20 close stars *with a similar distance modulus*; depending on the stellar density and number of measurements

³One could also use the more recent catalog by Heiles (2000) which contains observations for over 9000 stars.

in the catalog, this led to the selection of a region between 1 and 15° in radius around the target.

The stars selected from the catalog are used to find the ratio $P/E(B - V)$, and finally, based on an extinction value for our target and assuming this extinction is of interstellar origin only, an estimate of the interstellar polarization for the target is calculated, along with the average interstellar polarization angle. This angle is calculated with a simple average and with a distance-weighted average of the polarization angles of all the stars selected. If the alignment is good over all of the region studied, the two values will be similar to within $\pm 10^\circ$; if they are very different, it means the alignment is not very good and it is harder to find an average interstellar polarization angle.

If the position angles for the interstellar polarization and for the target are different, it points to an intrinsic origin for at least part of the polarization measured. Intrinsic polarization is also deduced from polarimetric variability. Histograms and maps of the polarization and its position angle are also used to estimate the importance of interstellar polarization.

4. Variability tests

Since a majority of single PMS stars are variable polarimetrically (Bastien 1982; Drissen, Bastien, & St-Louis 1989; Ménard & Bastien 1992), we expected PMS binaries, and MWC 1080 in particular, to also be polarimetrically variable, either periodically or not. Various statistical tests were applied to check the polarimetric variability or stability of PMS binaries; the details of those variability tests and the results for all the binaries of our sample will be presented in future papers.

Many PMS binary stars show odd observations with polarization levels and/or position angles well below or above the bulk of the data, and MWC 1080 is no exception. These data were removed before testing for variability. We believe these observations were due to some eruption-like events or significant modifications in the circumstellar environment (formation/destruction of condensations, accretion events), and not because of an instrumental problem: a close examination of polarization observations taken over 5 years of non-polarized standard stars (84 observations), polarized standard stars (53 observations), and 3 stars that were followed for many consecutive hours (121 observations) did not show odd observations like the ones we repeatedly saw for PMS binaries in general, and MWC 1080 in particular (Manset 2000).

5. Periodic variations

In addition to stochastic polarimetric variability, which is a general property of single PMS stars, PMS binaries will also present periodic polarimetric variations caused by the orbital motion, even if in some cases the amplitude may be too small to be detected with currently available instruments or masked by non-periodic or pseudo-periodic variations. In the case of Mie scattering,

we have also shown (Paper II) that dust grains, which are the main producers of the polarization, are less efficient polarizers and produce smaller amplitude variations than electrons; this is an indication that periodic polarimetric variations could be more difficult to observe in PMS binaries than in, for example, hot stars surrounded by electrons, which can easily show variations of a few tenths of a percent (see for example Robert et al. 1990; Robert et al. 1992).

Using the known orbital period, we calculate the orbital phase for each observation of each star and plot P , θ and the Stokes parameters Q and U as a function of the orbital phase. When enough data are available, observations are represented as first and second harmonics of $\lambda = 2\pi\phi$, where ϕ is the orbital phase, $0 < \phi < 1$:

$$Q = q_0 + q_1 \cos \lambda + q_2 \sin \lambda + q_3 \cos 2\lambda + q_4 \sin 2\lambda, \quad (1)$$

$$U = u_0 + u_1 \cos \lambda + u_2 \sin \lambda + u_3 \cos 2\lambda + u_4 \sin 2\lambda. \quad (2)$$

The coefficients of this fit are then used to find the orbital inclination, using the first or second-order Fourier coefficients, although it is usually expected that second order variations will dominate (BME):

$$\left[\frac{1 - \cos i}{1 + \cos i} \right]^2 = \frac{(u_1 + q_2)^2 + (u_2 - q_1)^2}{(u_2 + q_1)^2 + (u_1 - q_2)^2}, \quad (3)$$

$$\left[\frac{1 - \cos i}{1 + \cos i} \right]^4 = \frac{(u_3 + q_4)^2 + (u_4 - q_3)^2}{(u_4 + q_3)^2 + (u_3 - q_4)^2}. \quad (4)$$

Non-periodic phenomenons such as eruptive events, transient stellar spots, variable accretion, and rearrangements of the circumstellar or circumbinary material can cause pseudo-periodic polarimetric variations that may mask the strictly periodic ones, especially if the observations are taken over many orbital periods, as is the case here.

When periodic variations are detected, we use a Phase Dispersion Method (Stellingwerf 1978) and a Lomb normalized periodogram algorithm (Press et al. 1997) to investigate the significance of this periodicity. The Phase Dispersion Method (PDM) is a least-squared fitting technique suited for non-sinusoidal time variations covered by irregularly spaced observations, and finds the period that produces the least scatter about the mean curve. The Lomb normalized periodogram (LNP) method is more powerful than Fast Fourier Transform methods for uneven sampling, but still assumes the curve is sinusoidal, which may not be always appropriate for the polarimetric observations presented here.

6. MWC 1080 = HBC 318 = V628 Cas

6.1. General characteristics

Herbig Ae/Be stars are the higher-mass counterparts ($2 M_{\odot} \lesssim M \lesssim 10 M_{\odot}$) to the T Tauri stars. These objects are also associated with nebulosity and surrounded by circumstellar material; for a review, see Catala (1989). The emission in IR and mm-wave spectral domains can be explained by the presence of disks, with possibly central holes, and of envelopes (Miroshnichenko et al. 1999).

MWC 1080 is a luminous Herbig Ae/Be object of the Be type with $4 \times 10^4 L_{\odot}$, and a strong wind (Henning et al. 1998). Its kinematic distance was determined to be 2.2 kpc (Levreault 1985), and confirmed by photometry of neighboring stars by Grankin et al. (1992). There is a third star $0''.76$ away, west of MWC 1080 (Leinert et al. 1994), and a poorly collimated Herbig-Haro flow (Poetzel, Mundt, & Ray 1992); the proposed outflow cavity has a position angle of $\approx 60^{\circ}$.

MWC 1080's spectrum is characterized by strong emission lines ($H\alpha$, $H\beta$, Fe II), some with P Cygni profiles, but few absorption lines (Herbig 1960; Poetzel et al. 1992). The strong emission lines imply the presence of a large amount of circumstellar gas in the system.

The emission-line profiles have P Cygni shapes which would indicate that the gaseous envelope of MWC1080 is rather nearly spherical or at least not highly flattened, implying a small contribution to the optical polarization. Moreover, from spectroscopic data (Corporon & Lagrange 1999), one could assume that the envelope is not very asymmetric. On the other hand, according to Hillenbrand et al. (1992), MWC 1080 would belong to the Group I Herbig Ae/Be stars, and thus have a geometrically flat, optically thick circumstellar accretion disk, with optically thin inner regions from the stellar surface up to several stellar radii. This classification could change if other sources (like the other component of this multiple system) included in the beams or apertures contribute significantly to the observed emission.

Harvey, Thronson, & Gatley (1979) have reported an extended far-infrared emission associated with this object. An $8.8 \mu\text{m}$ map by Deutsch et al. (1995) shows extended elliptical emission $4''$ or 4000 AU in diameter. At $100 \mu\text{m}$, the emission is also extended (Di Francesco et al. 1994). There is a bipolar molecular outflow (Yoshida et al. 1991).

MWC 1080 is an eclipsing binary with an orbital period of 2.886926 d (Grankin et al. 1992; Shevchenko et al. 1994). Since the photometric variations are close to sinusoidal (Grankin et al. 1992), it is thought that the masses are very similar. The asymmetric light curve and different height peaks indicate an eccentric orbit with $e \approx 0.2 - 0.5$, whereas the moderate amplitude is due to a perceptible inclination of the orbital plane, i.e., the system is not seen exactly edge-on (Grankin et al. 1992).

Hillenbrand et al. (1992) measured a polarization of 1.79% at 75° in a V filter, estimated the interstellar polarization from neighboring stars to be 2.58% at 71° , therefore giving an intrinsic

polarization of 0.79%⁴. On the other hand, Garrison & Anderson (1978), using a different method, determined a different interstellar polarization of 2.00% at 168°, giving an intrinsic V polarization of 3.84% at 76°.

6.2. Polarimetric characteristics

6.2.1. Polarimetric observations

MWC 1080 was observed at the OMM (Canada) between August 1995 and June 1999, using a 8".2 aperture hole and a broad red filter (filter RG645 centered on 7660 Å, with 2410 Å FWHM). These data are presented in Table 1 where we give the Universal and Julian dates, the orbital phase, polarization and position angle along with their uncertainties.

The observations thus include the third star, located at 0".76 from the spectroscopic binary, or 1700 AU from the binary, assuming a distance of 2.2 kpc (Levreault 1985; Grankin et al. 1992). Since this star is located far away, it can contribute to the observations by adding a constant polarization, but it should not introduce variability unless it experiences some stochastic phenomenon such as flare-like eruptions or stellar spots.

Figure 1 presents these observations, with the polarization P , position angle θ and the Stokes parameters Q and U shown as a function of the orbital phase. The solid lines are the Fourier fits made according to Equations 1 and 2. As can be seen on that figure, MWC 1080 presents a few (4) observations which stand out from the rest of the data, and which were removed for the variability analysis and the fitting procedure (data from 1996, June 2, July 9, September 1 and 8). The data are also very noisy. The very deviant observations and the noise are not due to instrumental problems since observations for other stars are stable (see Section 4) and some of the observations for MWC 1080 consist of 2 – 5 individual measurements which are all consistent with one another.

We have also obtained data at the OPdM (France) in October 1996, using a V filter and a 10" aperture hole. These observations are presented in Table 2, along with data from the literature and OMM. The V observations from OMM and OPdM are presented in Figure 2. Observations were also obtained at OMM on 3 occasions at other wavelengths to produce curves of the linear polarization as a function of wavelength (see Table 3).

6.2.2. Interstellar and intrinsic polarization

An inspection of the Mathewson et al. (1978) catalog shows that MWC 1080 is in a region where the position angles are well aligned at 73 – 74° (simple and weighted averages of the position

⁴As given in their paper. See discussion in Section 6.2.2 concerning this subtraction.

angles for 51 stars found within 4° of MWC 1080 and having similar distance modulus), with a wide distribution of polarization values that go up to 5% (see Figure 3). This indicates that the interstellar polarization is strong in this region, and we estimate it to be, based on polarization for neighboring stars, $2.21 \pm 0.13\%$ at 73° in the V band, similar to the estimation by Hillenbrand et al. (1992) of 2.58% at 71° in the V band, but perpendicular to the Garrison & Anderson (1978) value of 2.00% at 168° . We believe, based on Hillenbrand et al.’s (1992) and our analysis of the Mathewson et al. (1978) catalog, that the interstellar polarization has a position angle of $\approx 75^\circ$ and not $\approx 165^\circ$.

Using our estimate of the IS polarization, 2.21% at 73° in the V band, and Serkowski’s law for interstellar polarization (Serkowski, Mathewson, & Ford 1975), we find an interstellar polarization value of 1.95 % at 73° at 7660 \AA . We have assumed that $\lambda_{\text{max}} = 5500 \text{ \AA}$ for Serkowski’s law (a typical value, and also a mean for 3 stars found near MWC 1080 in the Mathewson et al. (1978) catalog, and a value compatible with our wavelength-dependent data) and that the position angle of the interstellar polarization is constant as a function of wavelength.

From our data, MWC 1080’s average polarization is 1.60% at 81.6° at 7660 \AA ($N = 62$), and 1.96% at 76.4° at V ($N = 7$, data from OPdM and OMM only). Nine stars are found within 1° of MWC 1080. Two, at about half a degree, show polarization levels of 1.36% and 1.54%, with position angles of 62 and 63° , which indicates that a significant part of MWC 1080’s polarization is of interstellar origin.

A proper subtraction of the interstellar polarization from the observed polarization (using the Stokes parameters $Q = P \cos 2\theta$ and $U = P \sin 2\theta$ and not a usual vectorial subtraction as was apparently done in the Hillenbrand et al. (1992) paper, in particular in their table 2) gives estimates of the average intrinsic polarization for MWC 1080: 0.6% at 139° at 7660 \AA , and 0.35% at 142° in the V band. A proper subtraction taking the Hillenbrand et al. (1992) V data would give 0.84% at 152° ; Garrison & Anderson (1978) report a much higher and perpendicular polarization, 3.84% at 76° but we believe this is due to an inappropriate evaluation of the interstellar polarization.

The position angles $\approx 140^\circ$ trace the axis of symmetry of the system and are at about 90° with respect to the position angle ($\approx 60^\circ$) of the outflow cavity (Poetzel, Mundt, & Ray 1992), which is what is usually observed for PMS stars (Bastien 1988). We then confirm the Poetzel et al. (1992) scenario where the elongated structure they saw in the continuum at 7018 \AA is made of the innermost and brightest part of a reflection nebula, elongated in the outflow direction, and perpendicular to the polarization vector.

The significant intrinsic polarization indicates that the circumstellar or circumbinary material around this binary is arranged in an asymmetric geometry, for example, in a disk rather than a spherical shell.

Two other facts point to an intrinsic polarization component in the observed polarization for MWC 1080. First, MWC 1080 shows clear periodic variations (see below) that cannot be of interstellar origin. Second, the position angle of the polarization varies as a function of wavelength

(see below). Observations of polarized standard stars (whose polarization is of interstellar origin) by Schmidt, Elston, & Lupie (1992) show that the maximum observed rotation of the position angle for the wavelength range covered by our observations (4350–8580 Å) is $\approx 0.25^\circ$, much less than the $\sim 10^\circ$ rotation seen for MWC 1080.

As discussed by Dolan & Tapia (Dolan & Tapia 1986 and references cited), a wavelength-dependent position angle could in theory be attributed to multiple interstellar clouds containing different grain sizes magnetically aligned in different directions, or to an interstellar cloud where there is a continuous rotation of the grains’ orientation, but, once again, the variability argument points to the presence of intrinsic polarization.

6.2.3. Variability analysis

Already from Figure 1, it is obvious that MWC 1080’s polarization is variable. The detailed results of the variability tests for the 7660 Å wavelength and the *V* filter will be presented in a future paper, along with analysis for our other binaries. The analysis shows that MWC 1080 was clearly variable polarimetrically between August 1995 and June 1999, in both filters, with indications of variability on time scales of days and months.

The average polarization at 7660 Å for the period 1995–1999 is 1.6% at 82° , whereas unpublished data taken at the OMM on Jan. 15 1988 in the same filter and aperture hole show a significantly higher polarization value, $1.98 \pm 0.04\%$, but with a similar position angle, 81.7° . This points to long-term (years) variability.

Data for the *V* filter show that there might be a significant difference between observations taken before and after October 1973, as data from 1973 (Vrba et al. 1975) show a higher polarization and (slightly) different position angle. After 1973, the polarization and its angle seem to have stabilized, although there is still evidence of variability. In particular, the four observations taken at OPdM on 4 consecutive nights clearly show variability. Once again, this indicates that variability is present with different time scales.

On some nights (6), it was possible to get 3 observations within about 5 hours. On many occasions, a set of 3 points shows a systematic increase or decrease in polarization and/or position angle, usually by a significant amount, showing that the variations are not random. On other occasions, the position angle stayed constant. This indicates that variability is present on time scales of hours, as well as days, months, and years.

The variations in position angle are confined to within $\pm 5^\circ$ of the mean, which indicates that polarization variations are probably not due to a drastic change in the geometry of the circumstellar material, but rather to modifications in the density.

6.2.4. Periodic polarimetric variations

Figure 1 shows all the 7660 Å observations, and Figure 4 shows binned data, where the orbital phase has been divided in equal bins and the polarization data weight averaged; the error bars in Figure 4 are simple averages of the error bars of the data in each bin. Clear periodic variations with amplitudes in Q and $U \approx 0.1 - 0.2\%$ are seen, especially in polarization angle, but are not fitted well by the simple 1λ and 2λ sinusoidal curves; the coefficients for this fit are (Equations 1 and 2):

$$q_0 = -1.5229 \pm 0.0011 \quad (5) \qquad u_0 = 0.4536 \pm 0.0037 \quad (10)$$

$$q_1 = 0.0278 \pm 0.0014 \quad (6) \qquad u_1 = -0.0162 \pm 0.0049 \quad (11)$$

$$q_2 = -0.0260 \pm 0.0016 \quad (7) \qquad u_2 = -0.0141 \pm 0.0053 \quad (12)$$

$$q_3 = -0.0404 \pm 0.0015 \quad (8) \qquad u_3 = -0.0012 \pm 0.0051 \quad (13)$$

$$q_4 = 0.0430 \pm 0.0015 \quad (9) \qquad u_4 = -0.0587 \pm 0.0051 \quad (14)$$

Adding 3λ and 4λ harmonics does a better job (see Figure 5), but the fit is still not adequate; the coefficients for that fit are:

$$q_0 = -1.5189 \pm 0.0004 \quad (15) \qquad u_0 = 0.4557 \pm 0.0037 \quad (24)$$

$$q_1 = 0.0286 \pm 0.0005 \quad (16) \qquad u_1 = -0.0134 \pm 0.0051 \quad (25)$$

$$q_2 = -0.0309 \pm 0.0005 \quad (17) \qquad u_2 = -0.0162 \pm 0.0056 \quad (26)$$

$$q_3 = -0.0438 \pm 0.0005 \quad (18) \qquad u_3 = -0.0045 \pm 0.0053 \quad (27)$$

$$q_4 = 0.0376 \pm 0.0005 \quad (19) \qquad u_4 = -0.0625 \pm 0.0053 \quad (28)$$

$$q_5 = 0.0345 \pm 0.0005 \quad (20) \qquad u_5 = 0.0148 \pm 0.0053 \quad (29)$$

$$q_6 = 0.0083 \pm 0.0005 \quad (21) \qquad u_6 = 0.0169 \pm 0.0052 \quad (30)$$

$$q_7 = -0.0145 \pm 0.0005 \quad (22) \qquad u_7 = -0.0021 \pm 0.0050 \quad (31)$$

$$q_8 = 0.0118 \pm 0.0005 \quad (23) \qquad u_8 = -0.0038 \pm 0.0055 \quad (32)$$

The level of the the polarimetric variations could point to a circumstellar disk rather than a circumbinary disk, as we have shown in Paper II that the former configuration is more favorable to high amplitude variations. However, if we assume both stars in MWC 1080 have masses of $\sim 10 M_\odot$, the orbital period yields a separation of 0.1 AU between each star; if the radii are $\sim 5 R_\odot$, or about 0.025 AU, the photospheres are separated by only 0.05 AU, which does not leave much space for dusty circumstellar material (which might then just evaporate due to the proximity of the photospheres).

In the observed polarimetric curves, there are minima of polarization and maxima in position angle near phases 0.0 and 0.5. When the interstellar polarization, which is almost perpendicular to

the observed one, is removed from the observed polarization, the intrinsic polarization now shows a maxima near phases 0.0 and 0.5, close to the position of the primary and secondary eclipses (0.0 and 0.55 (Shevchenko et al. 1994)). Both 7660 Å and V observations show a sudden increase in intrinsic polarization around phase 0.5 (see Figures 2 and 4). Since this change is seen in both filters, it must be related to the eclipses. An increase in polarization during an eclipse is to be expected since shielding the unpolarized light from the star will increase the amount of the scattered (and polarized) light. Increase of polarization at phase 0.0 had already been detected in the U , B , and V bands by Shevchenko et al. (1994).

A prediction of our Paper I was that as the orbital eccentricity increases, the periodic variations start from pure double-periodic to include stronger and stronger single-periodic variations. The eccentricity for MWC 1080 is not known but is estimated to be between 0.2 and 0.5 (Grankin et al. 1992); the strength of double-periodic variations, which have amplitudes between 1.4 and 2.5 times those of the single-periodic one, would favor an eccentricity nearer to 0.2 than to 0.5, but the polarimetric curves can not be formally inverted to find the orbital eccentricity.

In addition, non-periodic variations introduce noise that contributes, sometimes substantially, to both harmonics, so that such a straightforward association between eccentricity and presence of 1λ variations cannot be made. We have shown in Papers I and II that factors other than eccentricity (time-varying optical depth, non equal luminosity stars, asymmetric geometries, scattering on dust grains) can also introduce such single-periodic variations.

The PDM finds periods of 1.1 and 2.5 d when we look at a subset of the data taken over a few months only, and the LNP shows a peak at 1.6 d which becomes significant (more than 97% chance that the data do not come from random Gaussian noise) when we look at the binned data. The periods of 1.6 d and 2.5 d could be related to the orbital period of 2.88 d.

6.2.5. Polarization as a function of wavelength

On three occasions, in 1996, 1997, and 1998, data were obtained in order to get $P(\lambda)$, the polarization as a function of wavelength. Data are presented in Table 3 and Figure 6. The polarization and its position angle are clearly variable as a function of wavelength and time. The observed position angle generally decreases towards shorter wavelengths, by up to 10° between 4350 Å and 8580 Å. Changes of up to 10° are also seen from year to year. Variations like those have already been observed for T Tauri stars (Bastien 1981).

The change of polarization angle as a function of wavelength is mostly an intrinsic variation, since the interstellar polarization shows minute variations as a function of wavelength (once again, see Schmidt, Elston, & Lupie 1992). Also, a study of the variability of polarized standard stars (Bastien et al. 1988), where the variability might due to IS polarization variability, shows variations $\lesssim 5^\circ$, also below those seen for MWC 1080. We therefore believe that IS polarization variability would not be able to explain the change of position angle as a function of wavelength for MWC 1080.

As data taken during the same night at the same wavelength show, significant variations might have occurred during the time the $P(\lambda)$ was measured. Nonetheless, the 3 curves seem to be relatively consistent from one data set to the other. The polarization has a general bell shape usually associated with interstellar polarization and the Serkowski law (Serkowski, Mathewson, & Ford 1975). In particular, this interstellar curve has a peak at $\approx 5500 \text{ \AA}$, near the peak of MWC 1080’s curve, which indicates, as already stated, that MWC 1080’s polarization is in great part of interstellar origin.

Using our estimate of the IS polarization for the V band and Serkowski’s law, we can compute the IS polarization for the observed wavelengths, and subtract it to find the intrinsic $P(\lambda)$ (see Figure 7). Removal of the IS polarization moves the peak of polarization to a redder wavelength around 7000 \AA .

Using the numerical code presented in Papers I and II, we have computed a few $P(\lambda)$ curves for different grain composition and sizes. Even though the number of free parameters is too high to uniquely determine the composition and size of the grains from the observed $P(\lambda)$ curve, these curves can nonetheless give some insight into the environment for MWC 1080. Figure 8 presents 3 $P(\lambda)$ curves for astronomical silicate grains of radii $0.02 \mu\text{m}$, $0.1 \mu\text{m}$, and $0.2 \mu\text{m}$. It is immediately seen that the size of the grains has a profound impact on the morphology of that curve.

From our simulations, the circumbinary disk configuration does not produce variations of the polarization angle as a function of wavelength, but the circumstellar disk does, for certain orbital phases. The variations are small, $3\text{--}4^\circ$, but the dependence can be either increasing or decreasing toward the blue, depending on the orbital phase. Since MWC 1080 does show a variable polarization angle, it points to a circumstellar disk, or at least, to the presence of matter close to the stars.

Qualitatively, then, the polarization for MWC 1080 could be reproduced by astronomical silicate grains of small sizes, between $0.02 \mu\text{m}$ and $0.1 \mu\text{m}$, located close to the stars, in an asymmetric configuration.

7. Photometry

Photometric observations of the irregular variable MWC 1080 show periodic variations with normal light variations of 0.16 magnitudes in V , along with irregular variability with $\Delta V = 0.3$ magnitudes, which introduces scatter in the periodic variations (Grankin et al. 1992). An inspection of a catalog of $UBVRI$ photometry of T Tauri stars (Herbst et al. 1994) with its on-line database⁵ containing ≈ 1600 observations for this binary also reveals that the average magnitude for MWC 1080 can change from one epoch to another. Peak-to-peak variations are $0.2 - 0.3$ magnitudes in V , whereas the scatter is of the same order. This stochastic photometric variability is

⁵Available at <ftp://www.astro.wesleyan.edu/pub/ttauri/>

probably related to the stochastic polarimetric variability observed here.

We have tried to cross-correlate photometric observations taken from that database with our polarimetric observations, and find data obtained quasi-simultaneously. Due to the physical locations of the observatories, the closest observations are within 0.25 – 0.5 days of each other, which is a significant portion of the orbital period. Nonetheless, we found about half a dozen quasi-simultaneous observations, which do not show any clear correlation between brightness of the star and its intrinsic polarization.

8. Orbital inclination

One of the goals of these observations is to find the orbital inclination for this binary system. Since it is an eclipsing binary, the orbital inclination is known to be close to 90° , but the light curve also suggests some small departure from an edge-on configuration (Grankin et al. 1992). Since the orbit might be significantly eccentric ($0.2 < e < 0.5$, Grankin et al. 1992), we should consider the results of the BME formalism using both orders (Equations 3 and 4), which are $i(O1) = 56 \pm 8^\circ$ and $i(O2) = 102 \pm 2^\circ$.

If the orbital eccentricity is $e \approx 0.2 - 0.3$, both orders should give about the same inclination, which is not the case. If the orbital eccentricity is higher than ≈ 0.3 , only the first-order results should be used ($i(O1) = 56 \pm 8^\circ$), but this result is not compatible with an eclipsing system, although the separation between the two components is small.

In Paper I, we showed that the amplitude of the polarimetric variations and the stochastic noise (or, scatter of the observations about the mean polarimetric variations) must be considered first in order to see if the orbital inclination found from Equations 3 and 4 is meaningful or not. According to our noise criteria (found after adding different levels of noise in the polarimetric curves produced by our numerical simulations; see Paper I for more details), the noise present in MWC 1080’s data is too high (the scatter is $\approx 0.08\%$ in polarization, or 50% of the amplitude of the variations) to allow the BME formalism to be used. Even applying the same analysis to the binned data, less numerous but showing much less scatter, gives the same conclusion.

The data have to be of exquisite quality (high number of observations, clear variations, not much stochastic noise) in order for the inclination found with the BME formalism to be meaningful. In the case of hot stars, the variations are usually of higher amplitude (by a factor of ~ 3) with less scatter from intrinsic non-periodic variations, so that in those cases, the noise criteria indicates the BME results are meaningful.

9. Summary and conclusions

We have presented polarimetric observations of a young massive short-period binary star of the Herbig Ae/Be type, MWC 1080. The mean polarization at 7660 Å is 1.60% at 81.6° (or 0.63% at 139° if an estimate of the interstellar polarization is subtracted) and 1.96% at 76.4° in the *V* band. The significant intrinsic polarization points to an asymmetric geometry of the circumstellar or circumbinary environment. The 139° intrinsic position angle traces the axis of symmetry of the system and is perpendicular to the position angle of the outflow cavity ($\approx 60^\circ$).

Although the interstellar polarization is very strong in this region, MWC 1080’s polarization cannot be of interstellar origin only, for 3 reasons. First, the estimated interstellar polarization for this region is different than the observed one for MWC 1080. Second, the significant variability of the polarization as a function of time (especially on time scales of hours) cannot be explained by modifications in the interstellar medium. Third, the dependence of the position angle on the wavelength along with its variability cannot be attributed to the interstellar medium.

This polarization is clearly variable, at all wavelengths, and on time scales of hours, days, months, and years; this is not a surprise and was expected since many PMS stars, of the Herbig Ae/Be or T Tauri type, show such variations. In addition to that stochastic variability, there are periodic variations due to the orbital motion of the stars in their dusty environment. Although stochastic (non-periodic) polarimetric variations introduce noise and scatter around the mean variations, binning the numerous observations reveals clear periodic polarimetric variations, which follow the known orbital period. The periodic polarimetric variations of this binary star are the first phased-locked ones detected for a PMS binary star that the authors are aware of.

The amplitude of the variations point to a circumstellar disk rather than a circumbinary one, since, according to our numerical simulations, the second configuration does not produce significant variations. However, the stars are probably so close to one another that there is not much room left for circumstellar material.

The variations are not simply double-periodic (as produced by a simple model of 2 equal mass stars in a circular orbit, at the center of an axisymmetric circumbinary envelope made of electrons), but include single-periodic and higher order variations. The presence of single-periodic variations could be due to non equal mass stars (although photometric observations point to equal mass or similar mass stars), the presence of dust grains, an asymmetric configuration of the circumstellar or circumbinary material, or the eccentricity of the orbit (which is thought to be between 0.2 and 0.5). The available data are for the moment insufficient to say what is the predominant cause of those single-periodic variations, or to find the geometry or orbital eccentricity of this system.

MWC 1080 is an eclipsing binary with primary and secondary eclipses occurring at phases 0.0 and 0.55. The signatures of the eclipses are seen in the polarimetric observations. The primary eclipse coincides with maxima in intrinsic polarization and position angle in the 7660 Å data. In addition, both 7660 Å and *V* observations show a sudden increase in polarization around phase 0.5

where the secondary eclipse is located.

Most of the observations have been obtained at a wavelength of 7660 Å, but we have obtained additional *V* band observations, and also observations as a function of wavelength on 3 occasions. The $P(\lambda)$ curve has a bell-shape morphology which changes on a time scale of a year, with a maximum polarization at about 5500 Å, typical of the interstellar polarization; when the estimated interstellar polarization is removed, the peak in the $P(\lambda)$ curve is displaced towards ≈ 7000 Å. The position angle also depends on the wavelength, with a rotation of $\sim 10^\circ$ over ~ 4000 Å, and on time. Both MWC 1080's polarization and position angle are thus dependent on time and wavelength.

The intrinsic polarization and intrinsic $P(\lambda)$ curves are consistent with the presence of dusty material in the circumstellar environment. Although it is not possible to uniquely determine the composition and size of the dust grains, our observations would be compatible with astronomical silicate grains with sizes in the range 0.02 – 0.1 μm .

Photometry for this irregular variable star shows stochastic variations that introduce significant scatter in the photometric light curve, a characteristic also seen in our polarimetric data. No clear correlation between brightness and polarization was found.

The stochastic polarimetric variations mentioned before introduce so much scatter that the orbital inclination obtained with the BME formalism is unfortunately not meaningful. This example shows that polarimetric observations have to be of exquisite quality (high number of observations, clear variations, not much stochastic noise) in order to find the orbital inclination.

Data on about 2 dozen other spectroscopic binary young stars will be presented in future papers.

N. M. would like to thank the Conseil de Recherche en Sciences Naturelles et Génie of Canada, the Fonds pour la Formation de Chercheurs et l'Aide à la Recherche of the province of Québec, the Faculté des Etudes Supérieures and the Département de physique of Université de Montréal for scholarships, and P. B. for financial support. We would like to thank the Conseil de Recherche en Sciences Naturelles et Génie of Canada for supporting this research.

The authors gratefully acknowledge financial support from Université Joseph Fourier, Grenoble (1994 BQR grant B 644 R1), the Laboratoire d'Astrophysique de l'Observatoire de Grenoble, and the Observatoire Midi-Pyrénées for upgrade and maintenance of the STERENN polarimeter.

We would like to thank F. Ménard for taking the Pic-du-Midi observations, and E. Magnier for reading the manuscript.

REFERENCES

- Bastien, P. 1981, *A&A*, 94, 294
- Bastien, P. 1982, *A&AS*, 48, 153
- Bastien, P. 1988, in *Polarized Radiation of Circumstellar Origin*, ed. G. V. Coyne et al. (Vatican City: Vatican Observatory), 541
- Bastien, P. 1996, in *ASP Conf. Ser. 97, Polarimetry in the Interstellar Medium*, ed. W. G. Roberge & D. C. B. Whittet (San Francisco: ASP), 297
- Bastien, P., Drissen, L., Ménard, F., Moffat, A. F. J., Robert, C., & St-Louis, N. 1988, *AJ*, 95, 900
- Brooks, A., Clarke, D., & McGale, P. A. 1994, *Vistas in Astronomy*, 38, 377
- Brown, J. C., Mclean, I. S., & Emslie, A. G. 1978, *A&A*, 68, 415
- Catala, C. 1989, in *ESO Conf. Proc. 33, Low Mass Star Formation and Pre-Main-Sequence Evolution*, ed. B. Reipurth (Garching: ESO), 471
- Clarke, D., & Naghizadeh-Khouei, J. 1994, *AJ*, 108, 687
- Corporon, P. & Lagrange A.-M. 1999, *A&ASuppl.*, 136, 429
- Deutsch, L. K., Hora, J. L., Butner, H. M., Hoffman, W. F., & Fazio, G. G. 1995, *Ap&SS*, 224, 89
- Di Francesco, J., Evans, N. J., Harvey, P. M., Mundy, L. G., & Butner, H. M. 1994, *ApJ*, 432, 710
- Dolan, J. F., & Tapia, S. 1986, *PASP*, 98, 792
- Drissen, L., Bastien, P., & St-Louis, N. 1989, *AJ*, 97, 814
- Garrison Jr., L. M., & Anderson, C. M. 1978, *ApJ*, 221, 601
- Grankin, K. N., Shevchenko, V. S., Chernyshev, A. V., Ibragimov, M. A., Kondratiev, W. B., Melnikov, S. Yu., & Yabukov, S. D. 1992, *IAU Information Bull. on Variable stars* 3747
- Harvey, P. M., Thronson, H., Jr., & Gatley, I. 1979, *ApJ*, 231, 115
- Heiles, C. 2000, *AJ*, 119, 923
- Henning, Th., Burkert, A., Launhardt, R., Leinert, Ch., & Stecklum, B. 1998, *A&A*, 336, 565
- Herbig, G. H. 1960, *ApJS*, 43, 337
- Herbst, W., Herbst, D. K., Grossman, E. J., & Weinstein, D. 1994, *AJ*, 108, 1906
- Hillenbrand, L. A., Strom, S. E., Vrba, F. J., & Keene, J. 1992, *ApJ*, 397, 613

- Leinert, Ch., Richichi, A., Weitzel, N., & Haas, M. 1994, in ASP Conf. Ser. 62, The Nature and Evolutionary Status of Herbig Ae/Be Stars, ed. P. S. Thé, M. R. Perez, & P. J. van den Heuvel (San Francisco: ASP), 155
- Levreault, R. M. 1985, Ph.D. thesis, University of Texas at Austin
- Manset, N. 2000, Ph.D. thesis, Université de Montréal
- Manset, N., & Bastien, P. 1995, PASP, 107, 483
- Manset, N., & Bastien, P. 2000, AJ, 120, 413 (Paper I)
- Manset, N., & Bastien, P. 2001, AJ, in press (astro-ph/0108124) (Paper II)
- Mathewson, D. S., Ford, V. I., Klare, G., Neckel, TH., & Krautter, J. 1978, BICDS, 14, 115
- Ménard, F., & Bastien, P. 1992, AJ, 103, 564
- Miroshnichenko, A., Ivezić, Ž., Vinković, D., & Elitzur, M. 1999, ApJ, 520, L115
- Press, W. H., Teukolsky, S. A., Vetterling, W. T., & Flannery, B. P. 1997, Numerical Recipes in C, The Art of Scientific Computing, 2d edition (Cambridge: Cambridge University Press)
- Poetzel, R., Mundt, R., & Ray, T. P. 1992, A&A, 262, 229
- Robert, C., Moffat, A. F. J., Bastien, P., St-Louis, N., & Drissen, L. 1990, ApJ, 359, 211
- Robert, C., et al. 1992, ApJ, 397, 277
- Rudy, R. J., & Kemp, J. C. 1978, ApJ, 221, 200
- Schmidt, G. D., Elston, R., & Lupie, O. L. 1992, AJ, 104, 1563
- Serkowski, K. 1958, Acta Astronomica, 8, 135
- Serkowski, K. 1974, in IAU Coll. 23, Planets, Stars, and Nebulae Studied with Photopolarimetry, ed. T. Gehrels (Tucson: University of Arizona Press), 135
- Serkowski, K., Mathewson, D. S., Ford, V. L. 1975, ApJ, 196, 261
- Shevchenko, V. S., Grankin, K. N., Ibragimov, M. A., Kondratiev, V. B., Melnikov, S. Yu., Petrov, P. P., Shcherbakov, V. A., & Vitrichenko, E. A. 1994, in ASP Conf. Ser., 62, The nature and evolutionary status of Herbig Ae/Be stars (San Francisco: ASP), 43
- Stellingwerf, R. F. 1978, ApJ, 224, 953
- Topping, J. 1972, Errors of Observation and their Treatment (London: Chapman and Hall)
- Vrba, F. J. 1975, ApJ, 195, 101

Yoshida, S., Kogure, T., Nakano, M., Tatematsu, K., & Wiramihardja, S. 1991, PASJ, 43, 363

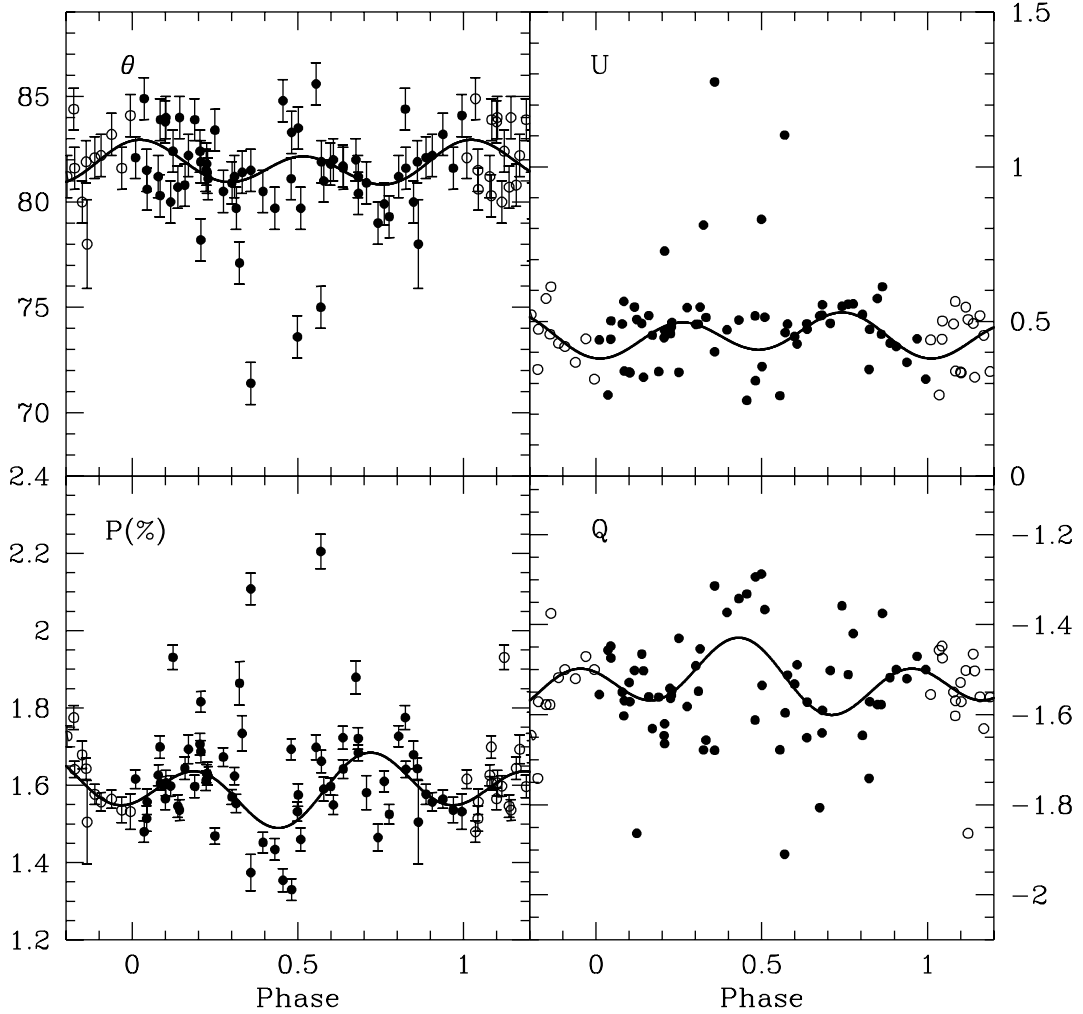


Fig. 1.— Complete set of polarimetric observations of MWC 1080, taken at 7660 \AA . The ephemeris used is from Grankin et al. (1992): $2445607.374 + 2.886926E$. The open circles are duplicates of filled circles and were added for clarity. A few observations are clearly away from the average curve, in both polarization and position angle, and are due to intrinsic variations. The solid line is the Fourier fit made according Equations 1 and 2. MWC 1080 is an eclipsing binary; the primary eclipse occurs at phase 0.0, and the secondary at phase 0.55.

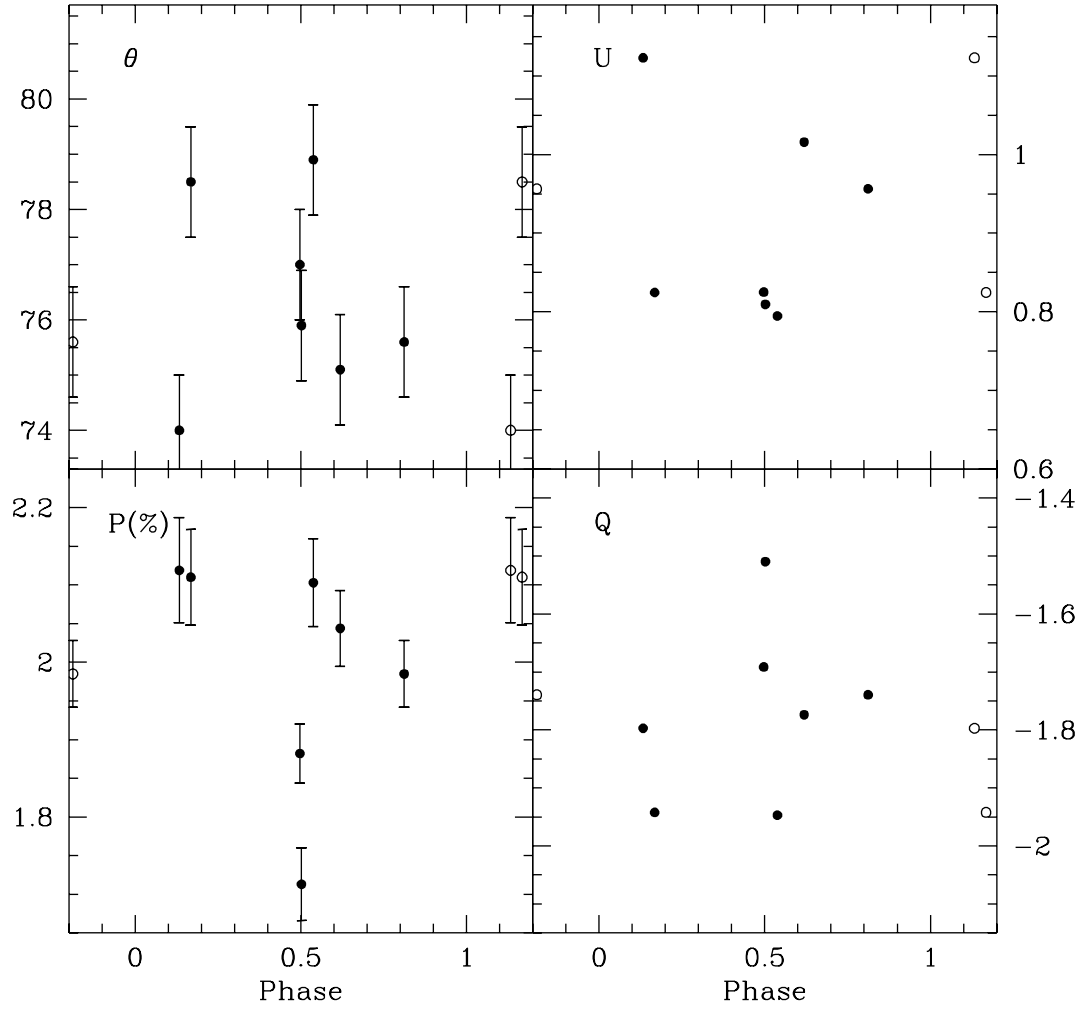


Fig. 2.— Polarimetric observations of MWC 1080, taken in the V filter at Pic-du-Midi and Mont Mégantic observatories. The ephemeris used is from Grankin et al. (1992).

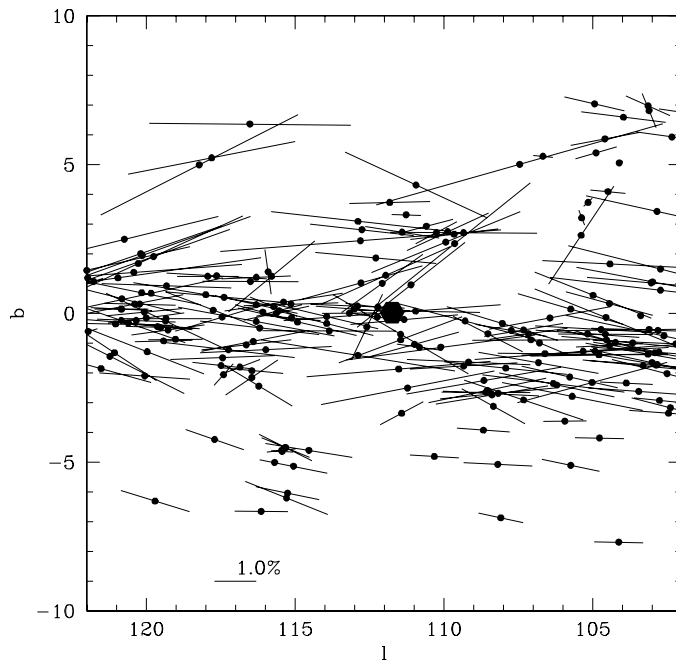


Fig. 3.— Interstellar polarization in the vicinity of MWC 1080, shown at the center of the field. Data are from the Mathewson et al. (1978) catalog.

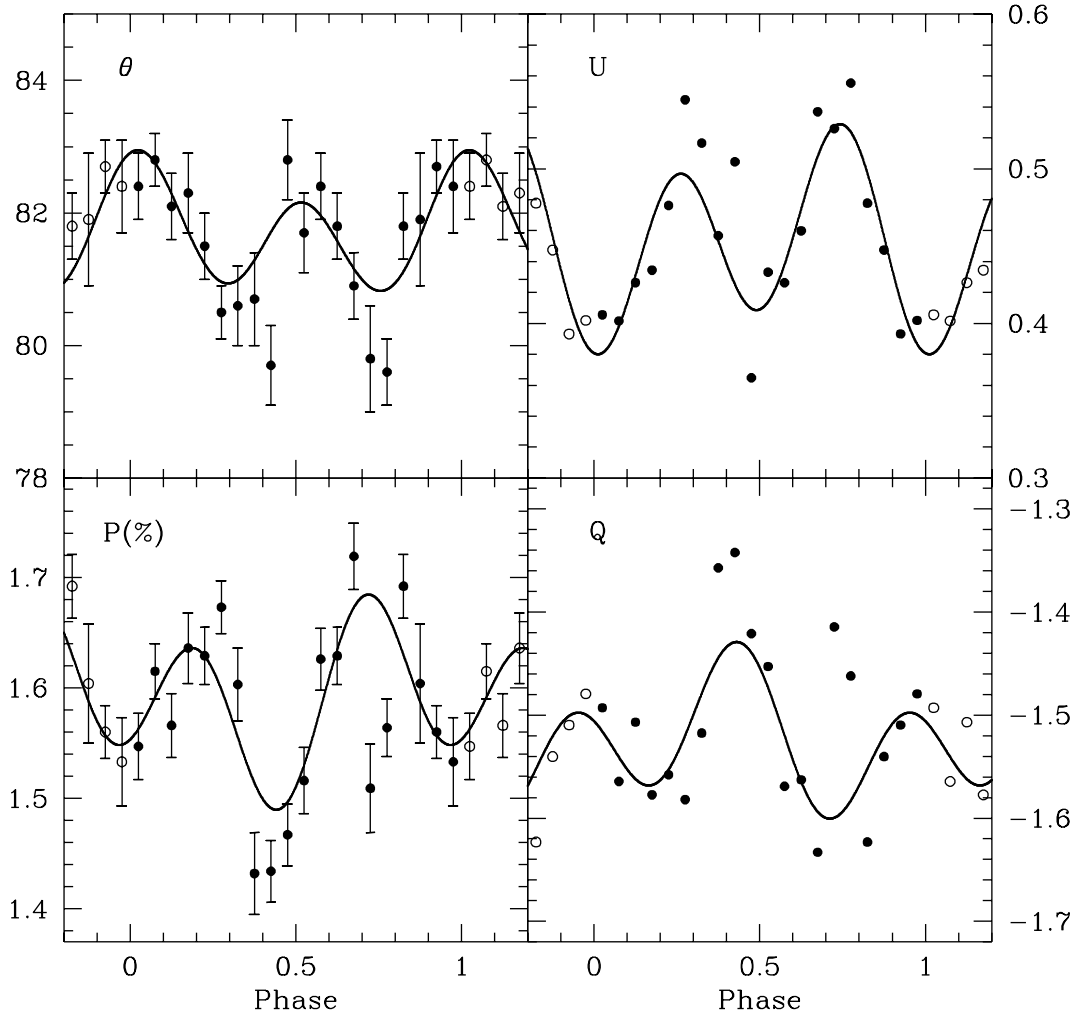


Fig. 4.— Binned polarimetric observations of MWC 1080. The most deviant points were removed before binning the data into 20 bins. Periodic variations are clearly seen. Note the steep change in polarization near phase 0.5.

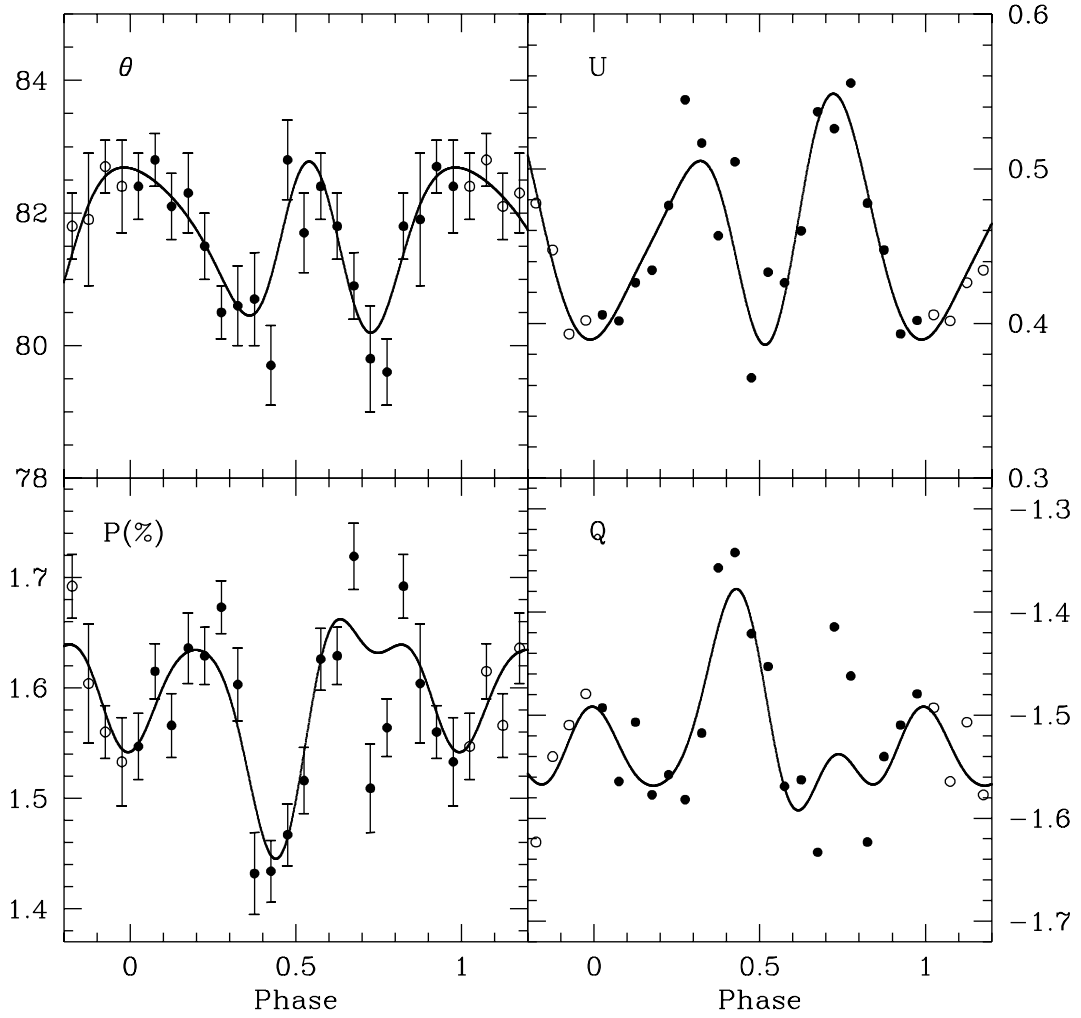


Fig. 5.— Binned polarimetric observations of MWC 1080, with an order 4 fit, showing that harmonics higher than second are present in the data.

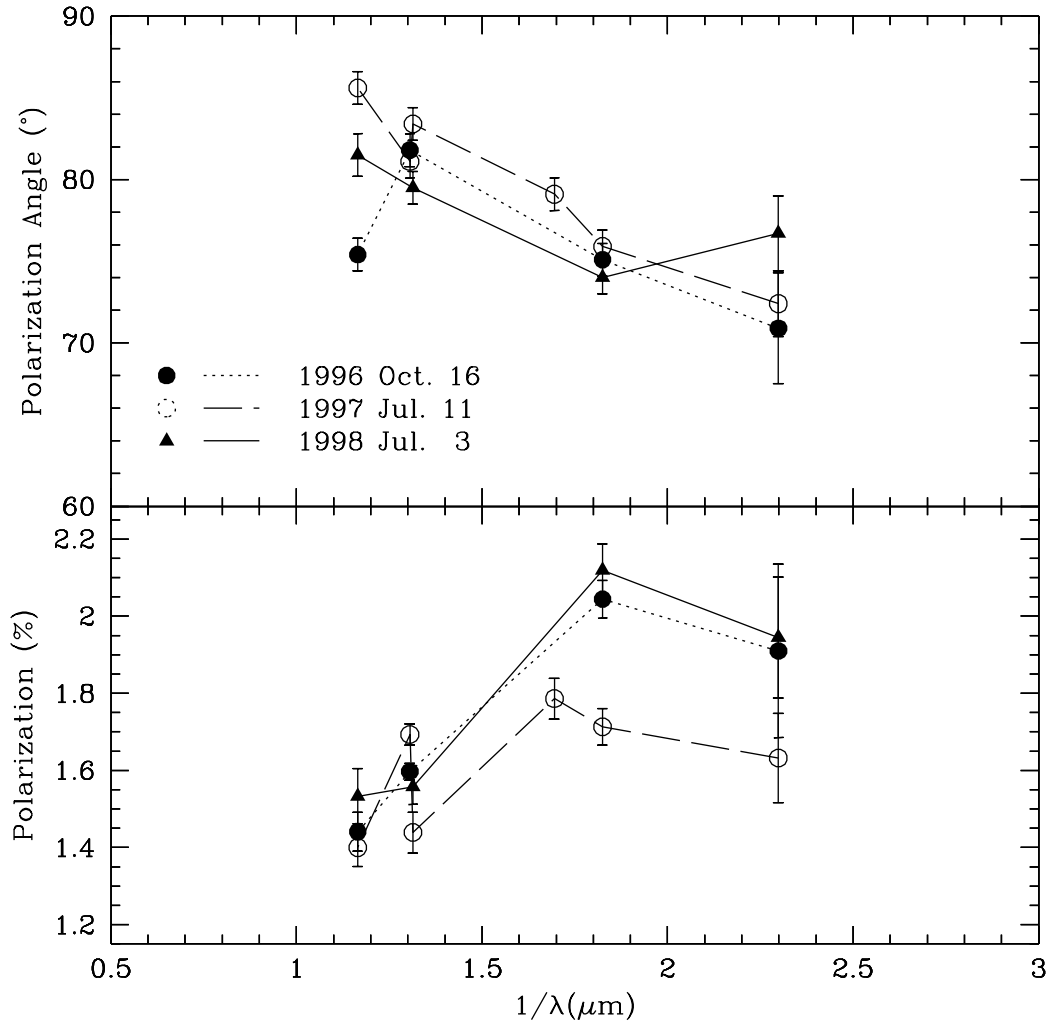


Fig. 6.— Observed polarization (intrinsic + interstellar) for MWC 1080 as a function of wavelength, for 3 different dates.

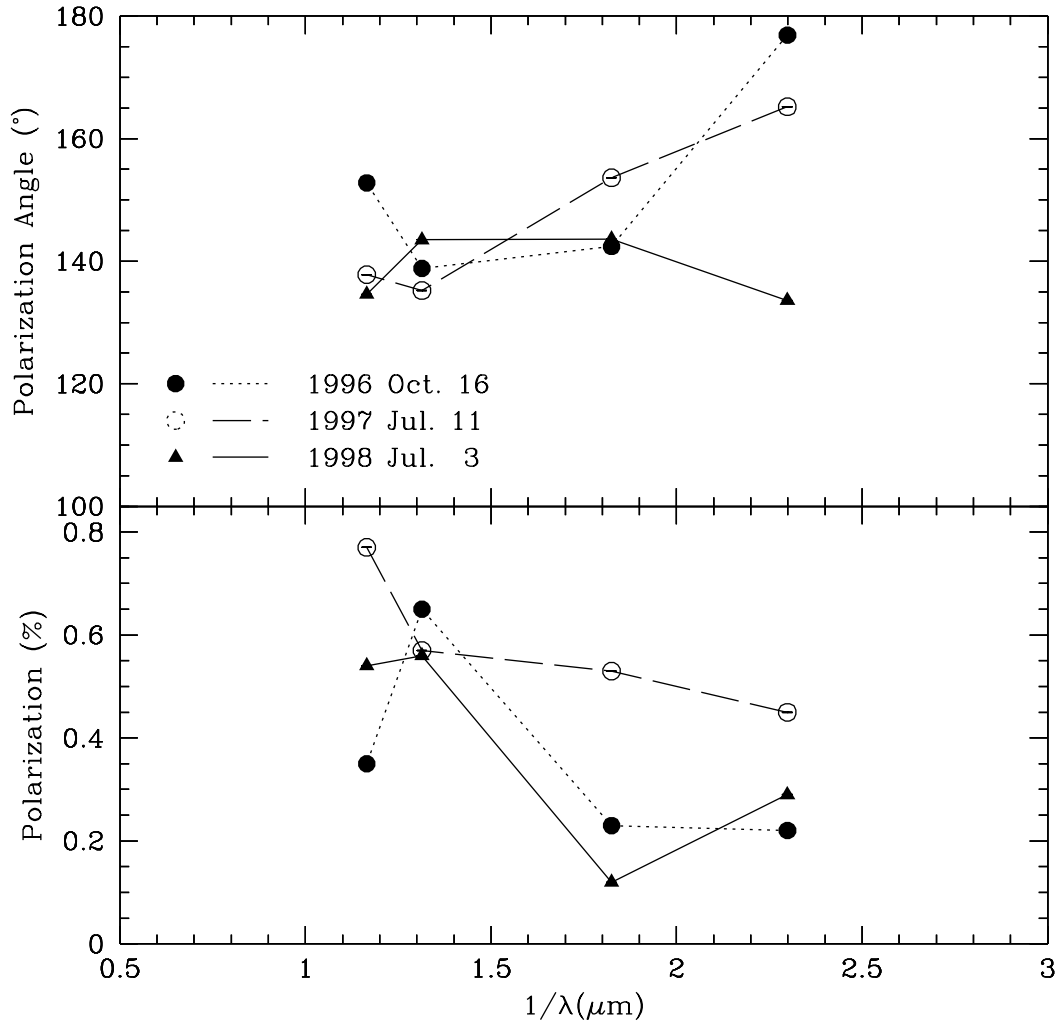


Fig. 7.— Intrinsic polarization for MWC 1080, after removal of the IS polarization. See text for more details.

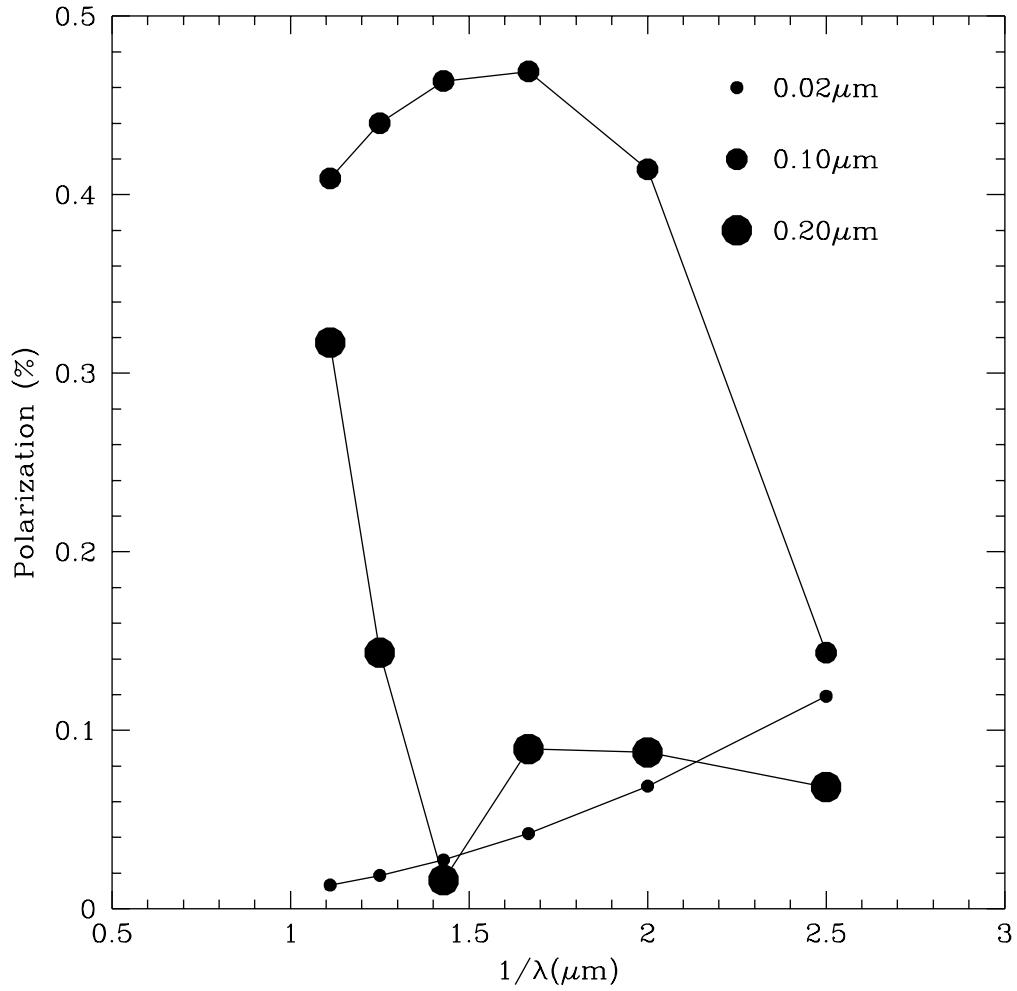


Fig. 8.— Polarization as a function of wavelength for astronomical silicate grains of radii $0.02 \mu\text{m}$, $0.10 \mu\text{m}$, and $0.20 \mu\text{m}$. Compare with the previous figure.

Table 1. Polarization data for MWC 1080, 7660 Å, Observatoire du Mont Mégantic

UT Date	JD 2400000.0+	Phase ¹	P(%)	$\sigma(P)$	$\theta(^{\circ})$	$\sigma(\theta)$
1995 Aug 17	49946.824	0.138	1.546	0.029	80.7	1.0
1995 Aug 19	49948.809	0.826	1.641	0.021	81.6	1.0
1995 Aug 26	49955.683	0.207	1.687	0.029	81.9	1.0
1995 Aug 28	49957.646	0.887	1.577	0.026	82.1	1.0
1995 Aug 29	49958.617	0.223	1.612	0.026	81.5	1.0
1995 Aug 31	49960.588	0.906	1.557	0.024	82.2	1.0
1995 Sep 2	49962.833	0.683	1.684	0.020	80.4	1.0
1995 Sep 3	49963.567	0.938	1.564	0.024	83.2	1.0
1995 Sep 3	49963.774	0.010	1.616	0.024	82.1	1.0
1995 Sep 4	49964.616	0.301	1.570	0.019	80.9	1.0
1996 Jan 1	50084.490	0.824	1.775	0.031	84.4	1.0
1996 Jan 3	50085.588	0.205	1.706	0.028	82.4	1.0
1996 Jan 4	50087.483	0.861	1.643	0.028	81.9	1.0
1996 Jan 7	50089.488	0.555	1.698	0.032	85.6	1.0
1996 Jun 1	50235.768	0.225	1.630	0.024	81.8	1.0
1996 Jun 2	50236.760	0.569	2.205	0.045	75.0	1.0
1996 Jun 2	50236.787	0.578	1.590	0.031	81.0	1.0
1996 Jun 12	50246.769	0.036	1.480	0.028	84.9	1.0
1996 Jul 9	50273.682	0.358	2.108	0.041	71.4	1.0
1996 Aug 24	50319.730	0.309	1.624	0.022	81.2	1.0
1996 Aug 25	50320.592	0.607	1.549	0.025	82.0	1.0
1996 Aug 25	50320.678	0.637	1.642	0.024	81.6	1.0
1996 Aug 25	50320.808	0.682	1.721	0.028	81.2	1.0
1996 Sep 1	50327.630	0.045	1.557	0.033	80.6	1.0
1996 Sep 1	50327.742	0.084	1.699	0.029	80.3	1.0
1996 Sep 1	50327.853	0.123	1.931	0.032	82.4	1.0
1996 Sep 4	50330.614	0.079	1.626	0.027	81.2	1.0
1996 Sep 4	50330.720	0.116	1.598	0.027	80.0	1.0
1996 Sep 4	50330.846	0.159	1.644	0.029	80.8	1.0
1996 Sep 6	50332.583	0.761	1.610	0.027	79.9	1.0
1996 Sep 7	50333.563	0.100	1.565	0.028	83.8	1.0
1996 Sep 7	50333.568	0.102	1.606	0.033	84.0	1.0

Table 1—Continued

UT Date	JD 2400000.0+	Phase ¹	P(%)	$\sigma(P)$	$\theta(^{\circ})$	$\sigma(\theta)$
1996 Sep 7	50333.685	0.143	1.536	0.027	84.0	1.0
1996 Sep 7	50333.820	0.189	1.597	0.029	83.9	1.0
1996 Sep 8	50334.587	0.455	1.354	0.030	84.8	1.0
1996 Sep 8	50334.715	0.499	1.532	0.025	73.6	1.0
1996 Sep 8	50334.721	0.501	1.575	0.029	83.5	1.0
1996 Oct 12	50368.637	0.250	1.469	0.021	83.4	1.0
1996 Oct 16	50372.532	0.599	1.597	0.022	81.8	1.0
1996 Dec 22	50439.523	0.804	1.727	0.027	81.2	1.0
1997 Jun 3	50602.791	0.358	1.374	0.047	81.5	1.0
1997 Jun 4	50603.799	0.707	1.581	0.044	80.9	1.0
1997 Jun 5	50604.772	0.044	1.514	0.033	81.5	1.0
1997 Jun 6	50605.784	0.395	1.452	0.027	80.5	1.0
1997 Jun 7	50606.786	0.742	1.465	0.035	79.0	1.0
1997 Jun 9	50608.774	0.431	1.434	0.028	79.7	1.0
1997 Jun 15	50614.773	0.509	1.460	0.030	79.7	1.0
1997 Jun 16	50615.756	0.849	1.679	0.036	80.0	1.0
1997 Jul 6	50635.753	0.776	1.525	0.025	79.3	1.0
1997 Jul 8	50637.788	0.481	1.330	0.028	83.3	1.0
1997 Jul 10	50639.777	0.170	1.693	0.037	82.2	1.0
1997 Jul 11	50640.674	0.480	1.693	0.027	81.1	1.0
1997 Aug 25	50685.723	0.085	1.605	0.017	83.9	1.0
1997 Sep 6	50697.623	0.207	1.816	0.027	78.2	1.0
1997 Sep 8	50699.823	0.969	1.536	0.033	81.6	1.0
1997 Sep 9	50700.575	0.229	1.624	0.024	81.1	1.0
1997 Sep 9	50700.707	0.275	1.673	0.024	80.5	1.0
1997 Sep 9	50700.820	0.314	1.553	0.024	79.7	1.0
1997 Oct 31	50752.532	0.227	1.630	0.030	81.4	1.0
1997 Nov 4	50756.600	0.636	1.723	0.030	81.7	1.0
1998 Jun 12	50976.666	0.864	1.505	0.108	78.0	2.1
1998 Jul 15	51009.749	0.324	1.864	0.056	77.1	1.0
1998 Aug 28	51053.765	0.571	1.662	0.029	81.9	1.0
1999 Jun 11	51340.795	0.995	1.532	0.046	84.1	1.0

Table 1—Continued

UT Date	JD 2400000.0+	Phase ¹	P(%)	$\sigma(P)$	$\theta(^{\circ})$	$\sigma(\theta)$
1999 Jun 12	51341.770	0.332	1.734	0.046	81.4	1.0
1999 Jun 13	51342.758	0.675	1.879	0.043	82.0	1.0

¹Calculated with the ephemeris $2445607.374 + 2.886926E$ (Grankin et al. 1992).

Table 2. Polarization data for MWC 1080, *V* filter

UT Date	Aperture	JD 2400000.0+	Phase ¹	P(%)	$\sigma(P)$	$\theta(^{\circ})$	$\sigma(\theta)$	Ref.
Oct 73	10''	2.54	0.3	68.2	...	1
Jan 76	13''	1.87	0.15	74	...	2
...	10''	1.79	...	75.0	...	3
1996 Oct 9	10''	50366.464	0.497	1.882	0.038	77.0	1.0	4
1996 Oct 10	10''	50367.373	0.812	1.985	0.043	75.6	1.0	4
1996 Oct 11	10''	50368.402	0.168	2.110	0.062	78.5	1.0	4
1996 Oct 12	10''	50369.470	0.538	2.103	0.057	78.9	1.0	4
1996 Oct 16	8''2	50372.589	0.619	2.044	0.049	75.1	1.0	5
1997 Jul 11	8''2	50640.738	0.503	1.713	0.047	75.9	1.0	5
1998 Jul 3	8''2	50997.649	0.133	2.119	0.068	74.0	1.0	5

¹Calculated with the ephemeris $2445607.374 + 2.886926E$ (Grankin et al. 1992).

References. — 1. Vrba et al. 1975; 2. Garrison & Anderson 1978; 3. Hillenbrand et al. 1992; 4. This paper. Data obtained at the Observatoire du Pic-du-Midi. 5. This paper. Data obtained at the Observatoire du Mont Mégantic.

Table 3. Polarization as a function of the wavelength

UT Date	JD 2400000.0+	Phase ¹	Filter	P(%)	$\sigma(P)$	$\theta(^{\circ})$	$\sigma(\theta)$
1996 Oct 16	50372.626	0.632	4350(990)	1.910	0.225	70.9	3.4
	50372.589	0.619	5480(1060)	2.044	0.049	75.1	1.0
	50372.532	0.600	7660(2410)	1.597	0.022	81.8	1.0
	50372.561	0.609	8580(630)	1.441	0.050	75.4	1.0
1997 Jul 11	50640.711	0.494	4350(990)	1.632	0.116	72.4	2.0
	50640.738	0.503	5480(1060)	1.713	0.047	75.9	1.0
	50640.787	0.520	5900(800)	1.786	0.053	79.1	1.0
	50640.808	0.527	7610(915)	1.439	0.053	83.4	1.0
	50640.762	0.511	8580(630)	1.400	0.049	85.6	1.0
1998 Jul 3	50997.712	0.155	4350(990)	1.945	0.157	76.7	2.3
	50997.649	0.133	5480(1060)	2.119	0.068	74.0	1.0
	50997.763	0.173	8580(630)	1.533	0.072	81.5	1.3
	50997.793	0.183	7610(915)	1.558	0.046	79.5	1.0

¹Calculated with the ephemeris $2445607.374 + 2.886926E$ (Grankin et al. 1992).